Quaternary Science Reviews, Vol. 11, pp. 181–189, 1992.
Printed in Great Britain.

0277–3791/92 $15.00

ESR DATING OF THE QUATERNARY DEEP-SEA SEDIMENT CORE RC17-177

Manfred Mudelsee, Michael Barabas and Augusto Mangini
Heidelberger Akademie der Wissenschaften, c/o Institut für Umweltphysik der Universität Heidelberg, Im Neuenheimer Feld 366, D-6900 Heidelberg, F.R.G.

The deep-sea sediment core RC17-177 from the west equatorial Pacific was dated with ESR using the signal at $g = 2.0036$ of foraminifera. The measured dose rate parameters were: U-, Th- and K-concentrations, ^{234}U- ^{230}Th- and ^{231}Pa-excess (initial values were assumed to be constant), average water content (derived from carbonate content) and a k_α-factor of 0.1 ± 0.02 (own experiment). The ESR-signal growth curves on γ-irradiation have been fitted by single exponential saturation functions. However, significant deviations from a single exponential form have been observed for larger γ-doses. Agreement between ESR ages from the signal at $g = 2.0036$ and those from an independent δ^{18}O stratigraphy was observed up to 800 ka. The existence of outliers could be explained by variable initial Th-excess or water content at different depths. On the contrary, the signal at $g = 2.0006$ delivered ADs (and corresponding ages) that are far too small due to a low thermal stability.

INTRODUCTION

The ESR dating method consists of the determination of the accumulated dose, AD, a sample has received and of the natural dose rate, P, at its burial site during the age, T. The age then can be derived from

$$\mathrm{AD} = \int_0^T P(t)\mathrm{d}t. \qquad (1)$$

It is expected that the ESR dating of sediment cores will deliver results to underpin U-series dating and to extend the dating range well beyond 300 ka. The studies that have been published so far about ESR-dating of deep-sea sediments (Sato, 1981, 1982; Takeuchi and Saeki, 1985; Mangini *et al.*, 1983; Siegele and Mangini, 1985; Barabas *et al.*, 1988), yielded the following results:

(a) There are three clearly distinguishable ESR signals in the foraminifera part of the sediment (which is the main part of the carbonate fraction) with g-factors at 2.0057, 2.0036 and 2.0006 (Fig. 1); all of them grow with the age of the sample up to at least 800 ka.

(b) The signals at $g = 2.0036$ and $g = 2.0006$ grow on γ-irradiation. Therefore both can in principle be used for the conventional additive dose method. However, while earlier studies assumed a linear growth, more recent observations (Barabas *et al.*, 1988) revealed a saturation like pattern of their growth curves.

(c) ESR ages derived from the signal at $g = 2.0006$ are systematically too young compared to δ^{18}O ages (Barabas *et al.*, 1988), whereas the ages from the signal at $g = 2.0036$ yielded corresponding results (ibid.).

(d) The signal at $g = 2.0036$ was found to be bleachable by light (Sato, 1983), depending on the wavelength used (Bettinger, *pers. commun.*). Although we could verify this effect in principle, storage for 1 week at the day light revealed no remarkable effect (Siegele, 1985). We assume that the usual procedure of storing (in darkness) and measuring the foraminifera has no remarkable effect on the signal intensity. This was corroborated by our results (see below).

Although sediment cores have important advantages for the use for ESR dating (a depth scale of chronological order, constant temperature and chemistry, infinite matrix assumption), the results quoted are more or less at the stage of 'relative' dating attempts as the accuracy for a certain AD determination was very poor and linear extrapolations have been used or some parameters have been adapted to fit the known δ^{18}O ages.

The aim of this study was: (1) to date a sediment core by ESR at the highest precision possible, i.e. to measure all dose rate parameters and the AD carefully for each depth up to an age of 800 ka; (2) to compare these independent ESR ages with a reliable δ^{18}O stratigraphy and to investigate systematic deviations.

These expectations, however, could not be fulfilled totally as the water content of the sediments — an important factor influencing the dose rate — could only be estimated with a rather large uncertainty.

SAMPLE MATERIAL

The deep-sea sediment core RC17-177 originates from a region of the west equatorial Pacific (Salomon Rise; 1°45.3′N, 159°26.9′E; 2600 m water depth; Shackleton, 1987). Forty samples from different depths (maximum 11.30 m) of this core consisted of cleaned, selected foraminifera (150–400 μm). Additional sediment material from the surroundings of the samples was available in most cases.

A δ^{18}O stratigraphy (Shackleton, *pers. commun.*) revealed a nearly constant sedimentation rate (1.2 cm/ka) and a maximum age of 766 ka at the basis of the core.

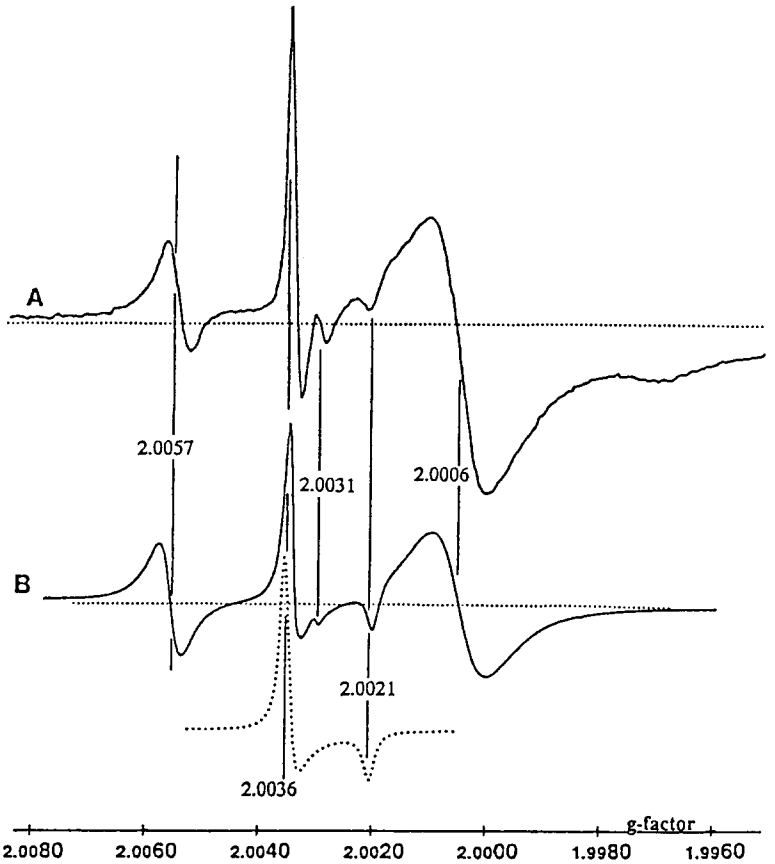

FIG. 1. ESR spectrum of foraminifera, measured (A) and simulated (B). The radiation-sensitive signals at $g = 2.0036$ (dotted line) and 2.0006 are used for dating.

DETERMINATION OF THE DOSE RATE

General Assumptions, Sources of the Natural Dose Rate

An infinite matrix radiation field was assumed, i.e. it was not distinguished between internal and external contributions. This seems to be reasonable as the range of the natural radiation (originating mainly from the surrounding sediment and material inside the foraminifera chambers) is large compared to the dimensions of the foraminifera walls (about 10 μm). This is valid even for α-particles with ranges between 13 and 35 μm (Brennan and Lyons, 1989).

The concentrations of ^{238}U and ^{232}Th have been measured by α-spectrometry. The ^{238}U-series usually contributes the largest part of the dose rate. The concentration of ^{235}U was assumed to be 1/138 of that of ^{238}U. ^{40}K was measured by flame photometry. Results are shown in Table 1. ^{87}Rb was neglected due to the small concentrations of K and the geochemical similarity of Rb to potassium (Warren, 1978). The cosmic radiation, which is shielded by the water column, and ^{14}C do not contribute to the natural dose rate.

The dose rates were calculated using the conversion tables of Nambi and Aitken (1986).

Radioactive Disequilibria

The assumption of a constant dose rate requires secular equilibrium in the decay chains of the long-lived nuclides ^{238}U, ^{235}U and ^{232}Th. However, in the case of deep-sea sediments the equilibria are disturbed at several decay steps. This effect causes the dose rate to be time dependent. These disequilibria are generated at the sedimentation process (initial disequilibria), they reduce with age with the life time of the respective nuclides.

^{234}U: The main fraction of carbonate-rich sediments is formed in the ocean water with an activity ratio $^{234}U/^{238}U$ of 1.14. This value was adopted for the initial sediment ^{234}U-excess.

^{230}Th: The largest disequilibrium in the sediment is due to the excess ^{230}Th which originates from preferential scavenging of ^{230}Th from the water column and transport into the sediment by sinking particles as compared to ^{234}U. Figure 2 shows the decay of the Th-excess for RC17-177 against the ^{18}O ages. We assumed for all depths a value of 5.50 ± 0.37 dpm/g for the initial excess ^{230}Th-concentration. This assumption is a possible source of systematic errors.

^{231}Pa (originating from ^{235}U): It shows a similar behaviour to ^{230}Th. Because of the low counting rate of ^{231}Pa its value was estimated from the initial excess ratio of $^{231}Pa/^{230}Th$ (about 1/22 in the western Pacific (Mangini, 1984)). However, the influence on the dose rate is small.

Alpha-Efficiency

Because of the high energy density along their tracks, α-particles are not as effective as β- or γ-particles in generating paramagnetic centres (see e.g. Zimmerman, 1972). This reduces the α-dose rate by the factor k_α, that is a function of the α-energy (ibid).

The α-dose of the natural decay chains contributes a large fraction to the natural dose rate. As no values for foraminifera have been published so far, a fine-grain experiment (see Zimmerman 1971, 1972) was carried out.

Sub-recent foraminifera from RC17-177 were annealed (2 hr at 200°C) to remove all signals. The sample was pounded and the remaining ESR signal was measured. By using a high microwave power (50 mW) the interference of the line at $g = 2.0006$ with the surface signal at $g = 2.0001$ (Lyons, 1988) was minimized. One fraction of the sample was γ-irradiated with ^{60}Co (198 Gy), the other part α-irradiated with a ^{241}Am source (1051 Gy, energy of impact 3.7 MeV). The different increases of the signals yielded k_α-factors with respect to the reference energy of 3.7 MeV: k_α (2.0036, ref.) = 0.123 ± 0.012, k_α (2.0006, ref.) = 0.109 ± 0.014. These values differ from each other only at a level of 45% significance.

Since the release of α-energy per track length and the alpha-efficiency itself therefore depend on the energy of impact and since natural α-energies vary and differ from 3.7 MeV the values were corrected according to Lyons and Brennan (1989):

$$k_\alpha\ (2.0036) = 0.1 \pm 0.02$$

$$k_\alpha\ (2.0006) = 0.08 \pm 0.02.$$

These values are in the range of measured values in other carbonates (e.g. Grün, 1989).

Water Content

The sediment usually contains water which attenuates the dose rate the sample receives.

$$P_{wet} = P_{dry} \frac{1}{1 + H_{\alpha,\beta,\gamma} \frac{X}{100-X}},$$

where X = water content in wt.%, $H_\alpha = 1.49$, $H_\beta = 1.25$ and $H_\gamma = 1.14$ (e.g. Grün, 1989).

A typical water content of about 50% reduces the γ- and β-dose rates to less than half their values. This emphasizes the importance of measuring the water content in every individual depth.

However, as the water content has not been measured in this core it was only derived from an estimated $CaCO_3$ content of 74 ± 14%. This led to an approximate average water content of 55 ± 5% (Lyle and Dymond, 1976). Therefore variations of the water content occurring in different depths could not be taken into account and may cause important deviations from the expected age values (see below).

Dose Rate, Dose Accumulation: Time Dependency

From the concentrations of U, Th and K and the radioactive excess of ^{234}U, ^{230}Th and ^{231}Pa the time dependency of the dose rate (Fig. 3a) as well as the accumulation of the radioactive dose $\int P\,dt$ (Fig. 3b) can be derived, considering the α-efficiency and the water content. The dose rate can be separated into a constant and a time varying part, the last of which is generated by the excess concentrations.

DETERMINATION OF THE ACCUMULATED DOSE

ESR Measurements

The AD was determined by the additive dose method, i.e. by extrapolation of the signal growth curve of γ-irradiation to the dose axis (e.g. Grün, 1989).

A ^{60}Co-source was used for γ-irradiations (dose rate about 6 Gy/min). The samples have been irradiated successively to the following doses: 0, 24.6, 48.9, 73.0, 148, 224, 337, 506, 722, 1040, 1480, 2130, 3300, 4880 and 8090 Gy. The source calibration was checked several times by alanine dosimetry (GSF, München).

For ESR measurements (BRUKER ESP 300) the samples were filled into fused quartz tubes (inside diameter 3 mm). Approximately 70 mg material was necessary to cover the full height of the resonator. As only a few 100 mg of each sample were available the whole procedure had to be repeated for each radiation step. Samples had been usually stored in the dark to avoid any light bleaching at the signal at $g = 2.0036$.

Constant parameters: frequency approximately 9.6 GHz ('X-band'); magnetic field strength approximately 0.35 T; sweep width 2 mT; modulation frequency 100 kHz.

Variable parameters, $g = 2.0006$ (2.0036): microwave power 20 mW (5 mW); sweep time 300 sec (600 sec); modulation amplitude 0.1 mT (0.04 mT); time constant 1.25 sec (0.64 sec).

Normalization of the measurements to a foraminifera standard minimized the influence of long-term variations of spectrometer performance.

Functional Form of the Signal Growth Curve

It has been shown elsewhere (e.g. Grün, 1989; Barabas *et al.*, 1988) that the ESR signals in $CaCO_3$ grow with a saturation-type pattern. This was also observed during our measurements on foraminifera.

According to these results we used a single exponential saturation function to determine the AD values:

$$S = K\left[1 - \exp\left(\frac{\text{dose} + \text{AD}}{D_0}\right)\right], \qquad (2)$$

S = ESR signal, K = signal maximum and D_0 = saturation dose. Commercial software (Asyst Software Inc.) was used for the determination of the fit parameters and their respective standard errors.

TABLE 1. RC17–177; chemical analysis; measured ADs from both g-values and 4 different maximum doses; ESR ages from g = 2.0036 (Fig. 6)

RC17-177		Chemical analysis				Measured AD (Gy), g = 2.0036				Measured AD (Gy), g = 2.0006				ESR age
depth (cm)	^{18}O age (ka)	^{238}U (ppm)	^{232}Th (ppm)	^{230}Th (dpm/g)	K (%)	max. γ-dose (Gy) 8090	4880	3300	2130	max. γ-dose (Gy) 8090	4880	3300	2130	g = 2.0036 (ka)
9.0	6.3	1.32 ± 0.24	0.94 ± 0.22	5.21 ± 0.26	*0.20	80 ± 44	34 ± 19	21 ± 13	15 ± 13	54 ± 32	35 ± 25	18 ± 17	4 ± 9	12^{+10}_{-9}
41.0	22.2	0.52 ± 0.05	0.99 ± 0.13	5.13 ± 0.15	*0.20	102 ± 31	69 ± 11	65 ± 11	66 ± 13	106 ± 33	75 ± 14	72 ± 15	56 ± 10	57^{+18}_{-14}
62.0	37.9	0.98 ± 0.37	1.46 ± 0.17	5.83 ± 0.17	*0.20	109 ± 38	66 ± 9	67 ± 10	74 ± 10	92 ± 27	67 ± 10	64 ± 10	56 ± 9	55^{+29}_{-16}
92.0	68.2	0.53 ± 0.06	1.10 ± 0.16	4.04 ± 0.15	0.22	166 ± 38	116 ± 15	100 ± 10	91 ± 9	128 ± 38	90 ± 19	79 ± 18	58 ± 9	92^{+23}_{-17}
113.0	82.2	0.87 ± 0.13	0.98 ± 0.20	3.31 ± 0.18	*0.20	161 ± 35	115 ± 5	118 ± 5	114 ± 6	134 ± 41	95 ± 25	84 ± 24	58 ± 13	111^{+29}_{-20}
151.0	105.4	0.47 ± 0.05	1.25 ± 0.15	3.43 ± 0.12	*0.20	162 ± 34	123 ± 12	130 ± 13	115 ± 10	114 ± 29	91 ± 15	92 ± 16	72 ± 9	134^{+37}_{-27}
172.0	123.7	0.57 ± 0.07	0.92 ± 0.14	2.77 ± 0.12	0.20	183 ± 25	153 ± 15	155 ± 17	132 ± 12	135 ± 29	109 ± 16	99 ± 15	87 ± 14	173^{+55}_{-39}
205.0	152.2	0.43 ± 0.06	1.53 ± 0.16	1.85 ± 0.09	*0.20	116 ± 26	96 ± 16	113 ± 10	107 ± 10	111 ± 21	95 ± 13	99 ± 14	88 ± 13	113^{+29}_{-21}
215.0	154.6	0.72 ± 0.10	0.95 ± 0.10	1.79 ± 0.07	*0.20	207 ± 45	146 ± 5	147 ± 5	144 ± 6	114 ± 18	104 ± 15	109 ± 16	93 ± 13	165^{+44}_{-30}
232.0	177.2	0.33 ± 0.03	0.49 ± 0.05	0.66 ± 0.03	*0.20	244 ± 27	211 ± 17	199 ± 17	182 ± 17	134 ± 24	113 ± 10	112 ± 11	101 ± 9	387^{+136}_{-102}
251.0	198.4	0.94 ± 0.05	0.70 ± 0.08	1.29 ± 0.06	0.21	275 ± 43	220 ± 28	203 ± 28	162 ± 18	131 ± 17	123 ± 16	115 ± 15	94 ± 6	224^{+73}_{-55}
281.0	226.2	0.92 ± 0.08	0.70 ± 0.12	0.97 ± 0.07	0.20	234 ± 38	186 ± 19	168 ± 15	154 ± 14	125 ± 20	111 ± 15	106 ± 15	92 ± 12	184^{+52}_{-38}
313.0	247.6	1.80 ± 0.09	1.27 ± 0.12	1.67 ± 0.07	0.24	339 ± 44	278 ± 25	255 ± 23	259 ± 30	183 ± 39	144 ± 20	133 ± 20	115 ± 17	256^{+63}_{-51}
331.0	263.9	0.36 ± 0.03	0.53 ± 0.05	0.47 ± 0.03	0.24	245 ± 27	214 ± 13	217 ± 14	214 ± 18	147 ± 28	131 ± 23	132 ± 26	102 ± 15	456^{+126}_{-105}
353.0	300.0	1.11 ± 0.08	0.63 ± 0.13	0.65 ± 0.06	0.16	187 ± 37	154 ± 26	150 ± 29	144 ± 34	121 ± 23	103 ± 10	105 ± 11	95 ± 8	154^{+69}_{-50}
381.0	324.4	0.62 ± 0.06	1.29 ± 0.13	0.68 ± 0.05	0.18	274 ± 46	207 ± 16	197 ± 16	194 ± 20	158 ± 28	134 ± 16	128 ± 16	111 ± 12	286^{+88}_{-66}
401.0	335.7	1.06 ± 0.06	0.61 ± 0.07	0.74 ± 0.04	0.15	281 ± 30	252 ± 26	225 ± 24	188 ± 17	172 ± 41	160 ± 43	124 ± 36	78 ± 9	281^{+82}_{-64}
420.0	347.3	0.70 ± 0.10	1.01 ± 0.13	0.65 ± 0.05	*0.20	269 ± 41	217 ± 22	199 ± 20	197 ± 24	157 ± 25	135 ± 14	131 ± 14	117 ± 12	284^{+102}_{-74}

435.0	360.3	*0.63 ± 0.06	*0.76 ± 0.10		*0.20	268 ± 59	190 ± 20	194 ± 23	164 ± 17	166 ± 32	142 ± 19	145 ± 21	126 ± 18	255^{+90}_{-65}
457.0	385.0	0.55 ± 0.05	0.61 ± 0.10	0.52 ± 0.05	*0.20	315 ± 57	230 ± 21	214 ± 21	215 ± 26	168 ± 31	139 ± 14	137 ± 15	121 ± 11	398^{+137}_{-108}
475.0	403.0	*0.63 ± 0.06	*0.76 ± 0.10		*0.20	243 ± 40	184 ± 15	166 ± 8	166 ± 10	152 ± 17	149 ± 18	141 ± 18	123 ± 16	222^{+60}_{-43}
497.0	423.8	0.84 ± 0.07	0.91 ± 0.12	0.68 ± 0.05	*0.20	428 ± 44	382 ± 37	389 ± 46	415 ± 66	270 ± 45	234 ± 36	226 ± 40	266 ± 53	889^{+234}_{-209}
517.0	443.8	*0.63 ± 0.06	*0.76 ± 0.10		*0.20	239 ± 27	209 ± 15	224 ± 13	209 ± 14	150 ± 16	143 ± 16	140 ± 17	132 ± 18	370^{+101}_{-78}
535.0	469.0	*0.63 ± 0.06	*0.76 ± 0.10		*0.20	297 ± 41	261 ± 36	232 ± 35	199 ± 35	174 ± 34	169 ± 36	169 ± 40	141 ± 40	367^{+157}_{-121}
565.0	501.5	*0.63 ± 0.06	*0.76 ± 0.10		*0.20	323 ± 39	266 ± 19	253 ± 19	252 ± 25	226 ± 26	209 ± 23	198 ± 24	203 ± 29	498^{+138}_{-114}
580.0	516.9	1.59 ± 0.20	0.70 ± 0.12	0.70 ± 0.06	*0.20	356 ± 61	294 ± 44	286 ± 51	383 ± 56	216 ± 25	203 ± 22	201 ± 25	228 ± 29	457^{+158}_{-131}
599.5	532.1	*0.63 ± 0.06	*0.76 ± 0.10		*0.20	280 ± 31	247 ± 20	246 ± 24	270 ± 29	170 ± 19	164 ± 19	159 ± 20	161 ± 24	519^{+152}_{-127}
620.0	544.5	0.80 ± 0.05	0.73 ± 0.08	0.41 ± 0.03	0.17	293 ± 31	264 ± 23	260 ± 26	271 ± 34	179 ± 24	172 ± 24	160 ± 25	144 ± 25	489^{+139}_{-192}
655.0	566.3	*0.63 ± 0.06	*0.76 ± 0.10		*0.20	475 ± 86	343 ± 46	310 ± 45	371 ± 59	252 ± 37	224 ± 29	210 ± 29	208 ± 34	837^{+256}_{-230}
681.0	584.4	1.37 ± 0.05	0.61 ± 0.07	1.07 ± 0.05	*0.20	463 ± 62	372 ± 30	378 ± 36	385 ± 49	241 ± 30	231 ± 30	232 ± 34	215 ± 38	630^{+143}_{-129}
710.0	603.9	0.54 ± 0.10	0.53 ± 0.12	0.56 ± 0.06	*0.20	428 ± 62	372 ± 58	316 ± 52	341 ± 73	229 ± 42	218 ± 43	191 ± 41	172 ± 44	903^{+357}_{-311}
750.0	624.8	1.16 ± 0.24	1.36 ± 0.38	0.54 ± 0.12	*0.20	477 ± 55	400 ± 32	390 ± 38	411 ± 52	219 ± 29	215 ± 32	201 ± 32	199 ± 39	679^{+214}_{-168}
790.0	645.5	*0.63 ± 0.06	*0.76 ± 0.10		*0.20	560 ± 111	414 ± 75	339 ± 61	350 ± 77	263 ± 68	211 ± 55	153 ± 33	136 ± 31	853^{+316}_{-287}
835.0	665.6	0.70 ± 0.12	0.74 ± 0.15	0.39 ± 0.05	*0.20	571 ± 51	508 ± 47	490 ± 56	464 ± 74	291 ± 31	274 ± 30	242 ± 25	232 ± 29	1305^{+356}_{-302}
895.0	685.5	0.87 ± 0.07	0.89 ± 0.12	0.72 ± 0.05	*0.20	409 ± 49	341 ± 33	299 ± 25	314 ± 32	195 ± 28	184 ± 27	169 ± 27	161 ± 30	571^{+140}_{-121}
955.0	706.2	1.19 ± 0.07	0.82 ± 0.11	0.97 ± 0.06	*0.20	528 ± 52	455 ± 34	449 ± 40	422 ± 49	259 ± 30	240 ± 26	222 ± 25	203 ± 25	817^{+173}_{-152}
1005.0	725.8	*0.63 ± 0.06	*0.76 ± 0.10		*0.20	479 ± 47	410 ± 31	393 ± 34	441 ± 45	247 ± 31	225 ± 28	206 ± 26	212 ± 32	1138^{+241}_{-210}
1040.0	740.1	*0.63 ± 0.06	*0.76 ± 0.10		*0.20	418 ± 39	359 ± 16	357 ± 19	362 ± 25	218 ± 25	208 ± 25	205 ± 27	214 ± 34	912^{+177}_{-151}
1075.0	754.4	0.73 ± 0.07	0.94 ± 0.11	0.46 ± 0.04	*0.20	355 ± 38	311 ± 26	315 ± 31	362 ± 26	216 ± 24	201 ± 22	196 ± 23	185 ± 26	734^{+176}_{-154}
1105.0	766.7	0.45 ± 0.04	0.83 ± 0.04	0.31 ± 0.01	*0.20	370 ± 36	315 ± 18	303 ± 19	278 ± 18	183 ± 22	169 ± 19	161 ± 19	156 ± 22	737^{+161}_{-138}

*Average value which was adopted when a sufficient amount of material was not available.

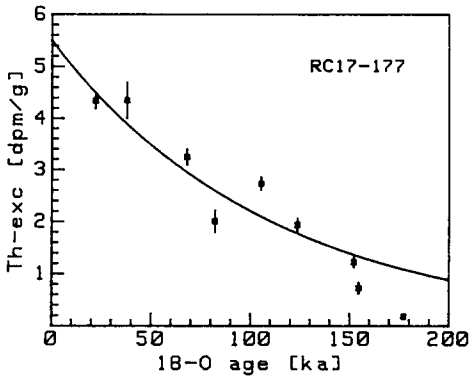

FIG. 2. Determination of the initial Th-excess for RC17-177. The values of the excess activities in separate depths are calculated from Table 1, subtracting the ^{234}U-activity from the ^{230}Th-activity: Th_{exc} (dpm/g) = ^{230}Th (dpm/g) − 1.38 ^{238}U (ppm) (1 + 0.15 exp($-\lambda_{234}t$)), λ_{234} = decay constant of ^{234}U. An exponential fit using the half-life of ^{230}Th yielded the initial value 5.50 ± 0.37 dpm/g. (Following Cochran and Osmond (1976), from the water depth, sedimentation rate, and a bulk density of 0.75 g/cm^3 (high carbonate content) a value of 7.4 dpm/g would result.)

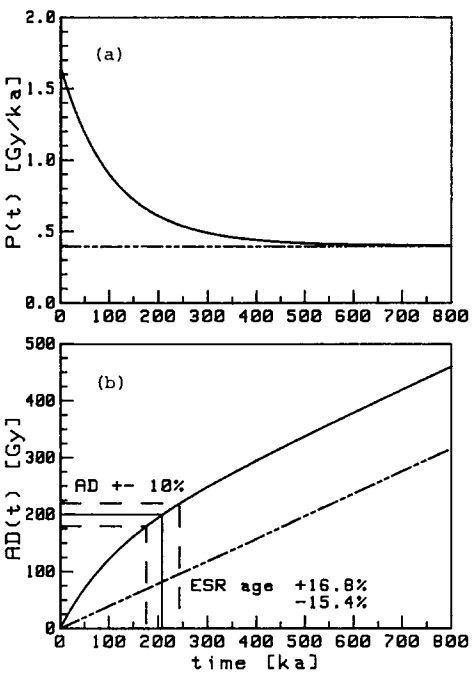

FIG. 3. RC17-177, typical progress in time of dose rate (a) and dose accumulation (b) $AD(t) = \int P(t)\,dt$. The solid line shows the original curves including the excess parts while the dashed one originates solely from a constant dose rate (no excess). Even after 800 ka the AD generated by the excesses has a notable portion. Figure 3b shows the deduction to the ESR age from a measured AD. Note that by the excesses the relative error of the AD (when projected on the time-axis) is enlarged and distorted.

RESULTS

AD-Dependency on ESR Signals

The ADs derived from the signal at g = 2.0006 are systematically smaller than those derived from g = 2.0036 (Table 1). These observations agree with earlier results (Barabas *et al.*, 1988).

As an independent check we *calculated* accumulated doses from the dose rate parameters and from the ^{18}O ages. These AD_{calc} have been compared with the *measured* (by ESR) AD_{meas} (Fig. 4) derived from each of the two signals.

The signal at g = 2.0036 gives AD_{meas} concordant to the AD_{calc} while ADs derived from g = 2.0006 are too small by about a factor of 2. Furthermore the ratio of AD_{meas} (g = 2.0006) and AD_{calc} tends to decrease with time which may indicate a low thermal stability (see Barabas *et al.*, 1992).

These findings confirm that the signal at g = 2.0036 is the appropriate dating signal, whereas — at least in the case of foraminifera — the signal at g = 2.0006 turned out not to be suitable for dating in this age range.

Thus for dating this sediment core we used the signal at g = 2.0036. The average standard deviation of the AD was about 11% (mean value of measurements).

The mean statistical uncertainty of the ADs derived from the signal at g = 2.0006 is not smaller. Thus it is unlikely that any remarkable influence of light in the case of the signal at g = 2.0036 has occurred, because this (random) effect would have increased the scattering of the signal growth curves.

Dependency on the Maximum Dose

Figure 5a shows two fits according to Eq. (2), one of which includes all 15 data points (maximum dose 8090 Gy), whereas the other excludes the point at the highest irradiation dose. A systematic difference was observed between the two fits, which can be expressed mathematically by decreasing parameters (maximum K, saturation dose D_0, AD) of the fit function with decreasing maximum dose. This tendency persists when using even lower maximum doses for the fitting procedure (i.e. eliminating the measured values that correspond to the respective highest dose). For example: at 8090, 4880, 3300, and 2130 Gy maximum dose the saturation dose for g = 2.0036 yields 1815, 1460, 1432, and 1322 Gy, respectively.

The enlargement (Fig. 5b) of Fig. 5a reveals the main consequence: the ADs derived from the best fit become significantly smaller with decreasing maximum dose. Example: the AD derived from g = 2.0036 for the maximum doses 4880, 3300, and 2130 Gy reduces in average by 23 ± 1, 27 ± 1, and 30 ± 1%, respectively, when related to 8090 Gy maximum dose (Table 1). Hence, the deviation of the signal growth curve from the single exponential saturation form is enlarged with growing irradiation steps. As a consequence this simple description of the signal behaviour is applicable only in lower regions of dose. Similar observations have been reported for molluscs (Katzenberger and Willems, 1988) and corals (Walther *et al.*, 1992). The reason for this behaviour may be the generation of new traps through irradiation (Aitken, 1985; Mitchell *et al.*, 1961; Grün, 1990).

Our assumption was that the smaller the dose range used for fitting the better is the approximation by a single exponential saturation function. That means the AD corresponding to the fit with the smallest maximum

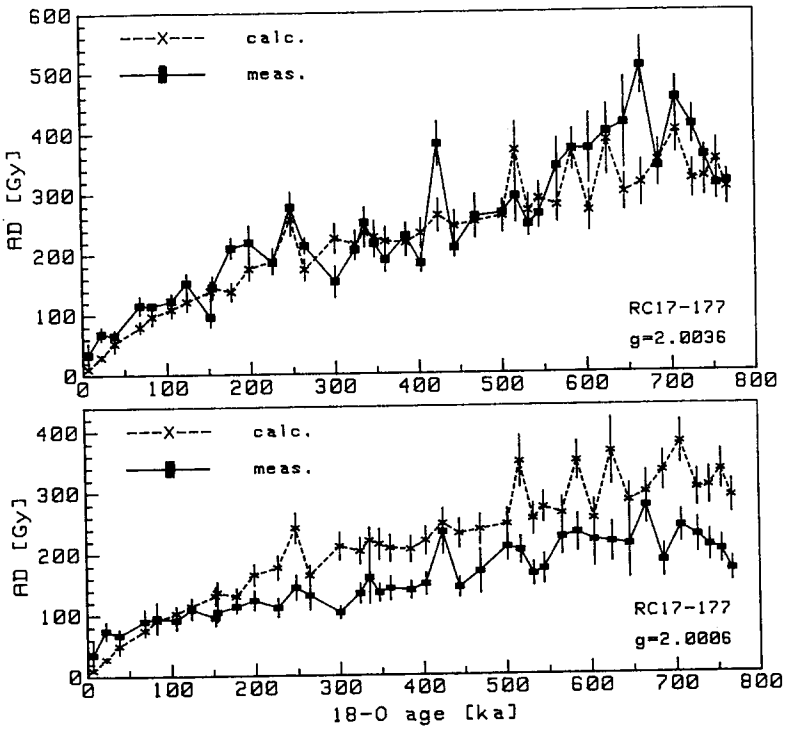

FIG. 4. ADs measured with additive dose method (4880 Gy maximum dose) and calculated with ^{18}O age and dose rate parameters. The measured ADs from the signal at $g = 2.0036$ show concordance while those from $g = 2.0006$ decrease with time against the calculated ADs.

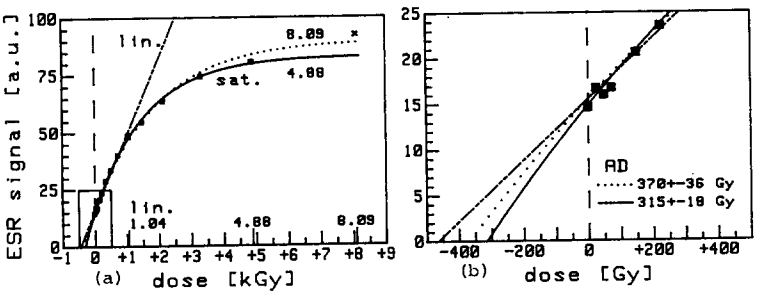

FIG. 5. RC17-177. (a) Typical signal growth curve (1105 cm, $g = 2.0036$) with a linear fit (10 data points, maximum dose 1040 Gy) and two saturation fits (15 points resp. 8090 Gy (dotted), 14 points resp. 4880 Gy (solid)). The enlargement (b) shows: (1) the linear fit overestimates the AD even when applied in lower regions of artificial dose; (2) the enhanced steepness (Fig. 3a) of the saturation fit at 8090 Gy maximum dose compared with that at 4880 Gy maximum dose has consequences for the AD also: a higher maximum artificial dose systematically leads to a higher value of the estimated AD.

doses comes closest to the true value. This assumption is supported by measurements on recent corals, shells and foraminifera by Walther *et al.* (1992) and Barabas *et al.* (1992). They showed that up to a dose range of about 1000 Gy the saturation function is a good enough description and yields only small systematic deviations for the AD determined.

On the other hand we could not eliminate more than four irradiation points, or else the statistical accuracy of the fit parameters (especially of the AD) would have become too poor. For a sufficient fit accuracy of the AD at least 10–15 data points and a dose range larger than the saturation dose D_0 (Barabas *et al.*, 1992) is recommended.

For AD determinations we used a maximum dose not exceeding 2000 Gy as a compromise between fit accuracy and systematic errors.

ESR Ages

Applying the conventional formula (see for example Grün, 1989) the ESR ages were calculated. This was done with a numerical approach because of the complexity of $P(t)$, i.e. the age cannot be expressed as a function of the other parameters explicitly. As shown in Fig. 6 — rough — concordance with $\delta^{18}O$ ages was attained within the whole time range up to 770 ka. No systematic deviation due to fading or bleaching was observed. Thus the life time of the signal at $g = 2.0036$ could be estimated to be at least 2 Ma.

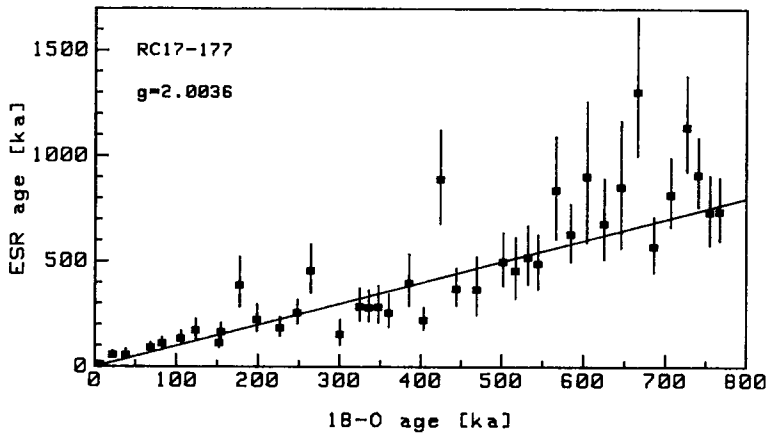

FIG. 6. ESR ages from the signal at $g = 2.0036$ in comparison with ^{18}O ages, 1:1 line. The ESR ages were determined using AD = ½ ($AD_{3300\,Gy\,maximum\,dose}$ + $AD_{2130Gy\,maximum\,dose}$) and 55% water content.

STATISTICAL ACCURACY

The ESR ages show an average error of 25%, when taking into account the standard errors assumed for every parameter. Error calculations include covariance terms since the parameters used are *not* independent statistically from each other.

Calculations showed that the main contribution (about 40%) to the overall *statistical* error of the ESR-ages is introduced by the uncertainty of the AD_{meas}. The next critical parameter is the water content, X, then uranium concentration, K_U, alpha-efficiency, k_α, and initial thorium excess, Th_{exc}. Additionally, the larger the initial excess concentration of ^{230}Th the larger will be the error of the ESR-age (Fig. 3b). The ^{232}Th-content can be neglected.

A χ^2-test, however, indicated systematic deviations between ESR and $\delta^{18}O$ ages. The extreme 'outliers' are listed in Table 2. We assumed that one (or more) of the parameters that can vary with depth may be responsible for these strong differences between ESR and $\delta^{18}O$ ages. In order to test this behaviour we calculated new values of these parameters sufficient to compensate the differences.

This led us to the following assessments:

— Fluctuations of the water content and/or initial Th-excess (both have been taken as constant for all depths), respectively, can be responsible for outlying ESR ages.

— Errors of the AD_{meas} are rather unlikely to explain the outliers.

— Incorrect U-measurements can be excluded, necessary concentrations would largely exceed the range of the measured values.

— The enormous deviations of the first sample (^{18}O age 22.2 ka, depth 41 cm) may be explained by processes in the upper layer, e.g. bioturbation.

— Bleaching effect seems very unlikely because most of the ESR ages of the outliers are too large.

CONCLUSIONS

(a) ESR dating of deep-sea sediments should be possible up to ages of at least 800 ka with an uncertainty of less than 20% using the signal at $g = 2.0036$ of foraminifera.

(b) The AD determination should involve saturation fits. When using a single exponential saturation function at least 12 data points should be available in a dose range not exceeding 2000 Gy since then the signal growth curve deviates from the single saturation form too strongly.

TABLE 2. Analysis of the 'outliers' in Fig. 6

^{18}O age (ka)	ESR age (ka)	Δ (σ)	X^* (%)	AD_{meas} (Gy)	AD^*_{meas}	Th^*_{exc} (dpm/g)	K_u (ppm)	K^*_u
22.2	57.3	2.52	10	66 ± 12	29	14.3	0.52 ± 0.05	8.0
177.2	387.0	2.05	38	191 ± 17	132	8.8	0.33 ± 0.03	1.8
263.9	456.1	1.84	44	216 ± 16	167	7.9	0.36 ± 0.03	1.2
300.0	153.9	−2.11	69	147 ± 32	219	2.1	1.11 ± 0.08	0.01
403.0	221.8	−3.04	66	166 ± 09	226	2.7	0.63 ± 0.06	< 0.00
423.8	889.3	2.22	33	402 ± 56	256	12.2	0.84 ± 0.07	2.5
665.6	1304.9	2.12	34	477 ± 65	306	13.2	0.70 ± 0.12	1.9
725.8	1138.4	1.96	42	417 ± 40	312	10.2	0.63 ± 0.06	1.3

The deviation Δ is measured in units of the standard error σ of the ESR age; an asterisk marks the parameters respectively necessary for equality of ESR and ^{18}O age; the values have to be compared with the true values $X = 55 \pm 5\%$, $Th_{exc} = 5.50 \pm 0.37$ dpm/g.

(c) Essential for the accurate determination of the dose rate are the measurements of the water contents and the uranium concentrations in each individual depth as well as the determination of the initial ^{230}Th-excess.

(d) Assuming the accuracies of U- and Th-measurements by neutron-activation-analysis to be 1%, an accuracy of water content measurements of 5%, a k_α-factor known within 5%, and AD determinations with 5% uncertainty (aliquots), a minimum statistical error of 15% for the ESR age would result.

(e) The signal at $g = 2.0006$ of foraminifera should not be used to determine ages that exceed 100 ka since it yields ADs (respective ages) that are clearly too small. The reason for this, we suppose, is the lower thermal stability of this signal (see Barabas *et al.*, 1992).

ACKNOWLEDGEMENTS

We gratefully acknowledge N.J. Shackleton (samples), U. Beck (U- and Th-measurements), H.-J. Lippolt (K-measurements), L. Zöller (α-irradiation), Universitätsfrauenklinik Heidelberg (γ-irradiation), MPI für medizinische Forschung Heidelberg for providing the ESR spectrometer and A. Wieser for providing alanine dosimeter and measurement time.

REFERENCES

Aitken, M.J. (1985). *Thermoluminescence Dating*. Academic Press, London, 359 pp.

Barabas, M., Bach, A. and Mangini, A. (1988). An analytical model for ESR-signals in calcite. *Nuclear Tracks and Radiation Measurements*, **14**, 231–235.

Barabas, M., Mudelsee, M., Walther, R. and Mangini, A. (1992). Dose–response and thermal behaviour of the ESR signal at $g = 2.0006$ in carbonates. *Quaternary Science Reviews*, **11**, 173–179.

Brennan, B.J. and Lyons, R.G. (1989). Ranges of alpha particles in various media. *Ancient TL*, **7**, 32–37.

Cochran, J.K. and Osmond, J.K. (1976). Sedimentation patterns and accumulation rates in the Tasman Basin. *Deep-Sea Research*, **23**, 193–210.

Grün, R. (1989). *Die ESR-Altersbestimmungsmethode*. Springer, Berlin, 132 pp.

Grün, R. (1990). Dose response of the paramagnetic centre at $g = 2.0007$ in corals. *Ancient TL*, **83**, 20–22.

Katzenberger, O. and Willems, N. (1988). Interferences encountered in the determination of AD of mollusc samples. *Quaternary Science Reviews*, **7**, 485–489.

Kennett, J. (1982). *Marine Geology*. Prentice-Hall, London, 813 pp.

Lyle, M.W. and Dymond, J. (1976). Metal accumulation rates in the southeast pacific — errors introduced from assumed bulk densities. *Earth and Planetary Science Letters*, **30**, 164–168.

Lyons, R.G. (1988). Dependence of accumulated dose in ESR dating on microwave power: a contra-indication to the routine use of low power levels. *Nuclear Tracks and Radiation Measurements*, **14**, 243–251.

Lyons, R.G. and Brennan, B.J. (1989). Alpha dose rate calculations in speleothem calcite: values of η and k_{eff}/k_{ref}. *Ancient TL*, **7**, 1–4.

Mangini, A. (1984). *Datierung von Sedimenten und andere Anwendungen der Radionuklide Th-230, Pa-231 und Be-10 in der marinen Geologie*. Habilitationsschrift, Fakultät für Geowissenschaften der Universität Heidelberg, 63 pp.

Mangini, A., Segl, M. and Schmitz, W. (1983). ESR studies on $CaCO_3$ of deep-sea sediments. *PACT*, **9**, 439–446.

Mitchell, P.V., Wiegand, D.A. and Smoluchowski, R. (1961). Formation of F Centers in KCl by X Rays. *Physical Review*, **121**, 484–498.

Nambi, K.S.V. and Aitken, M.J. (1986). Annual dose conversion factors for TL and ESR dating. *Archaeometry*, **28**, 202–205.

Sato, T. (1981). Electron spin resonance dating of calcareous microfossils in deep-sea sediment. *Rock Magnetism and Paleogeophysics*, **8**, 85–88.

Sato, T. (1982). ESR dating of planctonic foraminifera. *Nature*, **300**, 518.

Sato, T. (1983). Bleaching of ESR signals from planctonic foraminifera. *Rock Magnetism and Paleogeophysics*, **10**, 7–8.

Shackleton, N.J. (1987). Oxygen isotopes, ice volume and sea level. *Quaternary Science Reviews*, **6**, 183–190.

Siegele, R. (1985). *ESR Untersuchungen an marinen Karbonaten aus dem Quartär*. Diplomarbeit, Institut für Umweltphysik, Universität Heidelberg, 69 pp.

Siegele, R. and Mangini, A. (1985). Progress of ESR studies on $CaCO_3$ of deep-sea sediments. *Nuclear Tracks and Radiation Measurements*, **10**, 937–943.

Takeuchi, A. and Saeki, R. (1985). Electron spin resonance (ESR) signals of pelagic sediments in the Southern Pacific. *In*: Ikeya, M. and Miki, T. (eds), *ESR Dating and Dosimetry*, pp. 125–133. Ionics, Tokyo.

Walther, R., Barabas, M. and Mangini, A. (1992). Basic ESR studies on recent corals. *Quaternary Science Reviews*, **11**, 191–196.

Warren, S.E. (1978). Thermoluminescence dating of pottery: an assessment of the dose rate from Rubidium. *Archaeometry*, **20**, 71–72.

Zimmerman, D.W. (1971). Thermoluminescence dating using fine grains from pottery. *Archaeometry*, **13**, 29–52.

Zimmerman, D.W. (1972). Relative thermoluminescence effects of alpha- and beta-radiation. *Radiation Effects*, **14**, 81–92.